Expansion of a pulsar wind bubble in a binary system

Denis A. Leahy[1] and Brian Niebergal[1]

leahy@iras.ucalgary.ca, bnieber@iras.ucalgary.ca

ABSTRACT

The current work consists of numerical modeling of the expansion of the high pressure, low density cavity inflated by the energetic outflow from the pulsar inside the stellar wind environment provided by the stellar companion. In addition to modeling the pulsar bubble expansion, the diffusion loss equation is solved during the expansion. This give the evolution of the relativisitic electron population during the expansion and also the emission from the electrons, by synchrotron and inverse Compton processes.

1. Model Summary

A rapidly rotating pulsar injects magnetic field and relativistic particles into its pulsar wind nebula. The nebula is highly overpressured and hereafter is refered to as a bubble. The bubble and expands into its environment- the stellar wind of the early B-type companion star. Due to asymmetry in density in the stellar wind, the bubble expands more rapidly in the direction away from the companion. The asymmetry increases as the velocity of the outer end of the bubble increases, while the velocity of the inner end stagnates. The dynamics of the bubble expansion are described in the following sections.

2. Bubble Interior

The millisecond pulsar's wind has a termination shock at its contact with the external wind material. We model the dynamics of the resultant plerion or "bubble". The parameters chosen for calculation are based on the properties of the system LSI +61°303 . In the model there is constant energy injection inside a a strong stellar wind ($P_w \propto x^{-n}$ where $2.2 < n < 3.2$, typical for Be stars) which results in a bubble separated by the stellar wind by a thin surface containing all of the swept-up stellar wind material.

[1]Department of Physics and Astronomy, University of Calgary, Calgary AB, T2N 1N4, Canada

2.1. Magnetic Field Evolution

The magnetic field in the interior of the bubble evolves due to adiabatic expansion losses and injection from the pulsar. We assume a spatially uniform magnetic field due to the dominance of magnetic pressure and the high speed of sound in the bubble interior. First consider the case of adiabatic losses of the magnetic field but no injection. Due to flux conservation through an expanding cross-section of the bubble,

$$\Phi = \int_S \vec{B} \cdot d\vec{A} = B_r \cdot A$$
$$\frac{d\Phi}{dt} = 0 = \frac{dB_r}{dt} A + B_r \frac{dA}{dt} \tag{1}$$

Here the surface S is chosen (arbitrarily) to be on the equatorial plane. For the case of uniform expansion, volume expansion is related to area expansion by,

$$\frac{1}{3}\frac{dV}{V} = \frac{1}{2}\frac{dA}{A}$$

Which along with eq. (1) gives,

$$\frac{dB_r}{dt} = -\frac{2}{3}\frac{B_r}{V}\frac{dV}{dt} \tag{2}$$

The change in magnetic field due solely to energy injection (no expansion) can be found by considering a fixed inner boundary through which magnetic energy from the pulsar is being injected(see fig. **??**). We consider injection at a constant rate Choosing a cylinder of equal radius and height as the fixed boundary gives,

$$k_\Phi \equiv \frac{d\Phi_b}{dt} = \frac{dB_r}{dt} 3\pi R_b^2 \tag{3}$$
$$V = k_V R_b^3 \rightarrow R_b^2 = k_V V^{\frac{2}{3}}$$
$$\frac{dB_r}{dt} = \frac{k_\Phi}{3\pi k_V} V^{-\frac{2}{3}}$$

We want to use the components of the magnetic field that contribute to overall pressure, and we assume the field components on average are of equal magnitude.

$$\frac{dB}{dt} = \frac{2}{3}\frac{k_\Phi}{\pi k_V} V^{-\frac{2}{3}} \tag{4}$$

Adding the contributions from eqs. (2 & 4) gives,

$$\frac{dB_r}{dt} = -\frac{2}{3}\frac{B_r}{V}\frac{dV}{dt} + \frac{k}{V^{\frac{2}{3}}}$$

Multiplying by an integrating factor gives the solution,

$$B(t) = \left(kt + B_0 V_0^{\frac{2}{3}}\right) V(t)^{-\frac{2}{3}} \tag{5}$$

2.2. Momentum Equation and Pressure Balance

P_b is the bubble pressure due to magnetic field, and P_w is the primary star's wind pressure. For a given piece of the bubble's shell,

$$\frac{d}{dt}(mv) = \dot{m}v + \dot{v}m = \Delta A\,(P_b - P_w)$$

$$\rightarrow \dot{v} = -v\frac{\dot{m}}{m} + \frac{\Delta A}{m}\,(P_b - P_w)$$

The wind pressure is from $P_w = n_w k T_w$,

$$P_w = 2.158\left(\frac{10R_\odot}{x}\right)^{3.2}$$

The mass swept up by a shell piece of area ΔA is,

$$\dot{m} = \rho_w v_b \Delta A$$

Where ρ_w is the wind density,

$$\rho_w = \rho_0\left(\frac{x}{10R_\odot}\right)^{-n}$$

where ρ_0 is the density at $10R_\odot$, and x is the distance from the primary star to a point on the bubble surface. Now define a constant,

$$c = \rho_0\,(10R_\odot)^{-3.2}$$

Then we have two coupled differential equations,

$$\frac{d^2 r_b}{dt^2} = \frac{dv_b}{dt} = -\frac{c}{x^{3.2}}\frac{\Delta A}{m}v_b^2 + \left(\frac{B^2}{\mu} - P_w\right)\frac{\Delta A}{m} \tag{6}$$

$$\frac{dm}{dt} = \frac{c}{x^{3.2}}v_b \Delta A \tag{7}$$

where r_b is the radius of the bubble wall from the pulsar. These can be solved computationaly with the relations,

$$x = \sqrt{(z+L)^2 + \rho^2}$$

$$r_b^2 = z^2 + \rho^2$$

.

3. Diffusion Loss Equation Solution

There are three mechanisms for electron energy loss.

1 - Synchrotron Losses,

$$\frac{dE}{dt} = -a_s B^2 E^2$$

2 - Inverse Compton Scattering,

$$\frac{dE}{dt} = -a_c U_{rad} E^2$$

where U_{rad} is the radiation from the primary star,

$$U_{rad} = L_{rad}/4\pi c \left\langle x^2 \right\rangle$$

3 - Adiabatic Losses for a relativistic fluid,

$$dE = -P \cdot dV$$

$$P = \frac{1}{3}\frac{E}{V}$$

$$\frac{dE}{dt} = -\frac{1}{3}\frac{E}{V}\frac{dV}{dt}$$

Now define,

$$f_1 = a_s B^2 + a_c U_{rad}$$

$$f_2 = \frac{1}{3V}\frac{dV}{dt}$$

$$b = -\frac{dE}{dt}_{tot} = f_1 E^2 + f_2 E$$

The diffusion loss equation with the assumption of a well-mixed fluid is,

$$\frac{dN}{dt} = \frac{\partial}{\partial E}\left[b(E)N(E)\right] + Q(E)$$

$$\frac{dN}{dt} = \frac{\partial N}{\partial E}\frac{dE}{dt} + \frac{\partial N}{\partial t}$$

$$\left(2f_1 E + f_2\right) N(E) + Q(E) = -2\left(f_1 E^2 + f_2 E\right)\frac{\partial N}{\partial E} + \frac{\partial N}{\partial t} \tag{8}$$

Solving the eq. (8) using method of characteristics,

$$N\left(E(s), t(s)\right) => \frac{dN}{dt} = \frac{\partial N}{\partial E}\frac{dE}{ds} + \frac{\partial N}{\partial t}\frac{dt}{ds}$$

Relating the above equation with eq. (8) gives,

$$\begin{aligned} t &= s & (9)\\ \frac{dE}{ds} &= -2\left(f_1 E^2 + f_2 E\right) & (10)\\ \frac{dN}{ds} &= \left(2f_1 E + f_2\right) N(E) + Q(E) & (11) \end{aligned}$$

the second is a Bernoulli ODE and the third a linear ODE that have solutions,

$$E(t) = V(t)^{-\frac{2}{3}} \left(\int_t V(t')^{-\frac{2}{3}} 2 f_1(t') dt' + V_0^{-\frac{2}{3}} E_0^{-1} \right)^{-1} \quad (12)$$

$$N(t) = \frac{\int_t e^{\int_{t'} -2 f_1(t'') E(t'') dt''} V(t')^{-\frac{1}{3}} Q(E(t')) dt' + \left(V_0^{-\frac{1}{3}} H(E_0) \right)}{e^{-\int_t 2 f_1(t') E(t') dt'} V(t)^{-\frac{1}{3}}} \quad (13)$$

Which is solved given the output from the RK4 program (time, magnetic field, $\langle x^2 \rangle$, and volume). Where $\langle x^2 \rangle$ is defined by the volume averge,

$$\langle x^2 \rangle = \frac{1}{V} \sum_{i=1}^{N} V_i x_i^2$$

4. Results

The dynamical evolution of the pulsar wind bubble was calculated using one program and the solution of the diffusion-loss equation in another. The expansion of the bubble is illustrated in Fig. 3, which is for the set of parameters: injection rate $k = 3 \times 10^{15} T m s^{-1}$, density at $10 R_\odot$ $\rho_0 = 10^{-8}$, wind density exponent $n = 3.2$ and pulsar-companion separation $L = 5.85 \times 10^{10}$m (called the fiducial case). The plot is made in cylindrical coordinates with the cylinder axis along the x (horizontal) axis. The pulsar is at coordinates (0,0) and the companion star at (-100,0). The expansion starts out spherical but then becomes asymmetrical as the outer boundary (point on the bubble and x-axis which is furthest from the companion) moves more rapidly than the inner boundary (point on the bubble and x-axis closest to the companion).

Due to strong adiabatic, synchrotron and inverse-Compton losses, the particle population evolves rapidly in time. Fig. 4 shows how the energies of electrons decrease with time in the first few hundred seconds for the fiducial case and for a stellar photon luminosity of 10^{31} W. Above $\sim 10^{-13}$J, synchrotron losses dominate and below this energy adiabatic

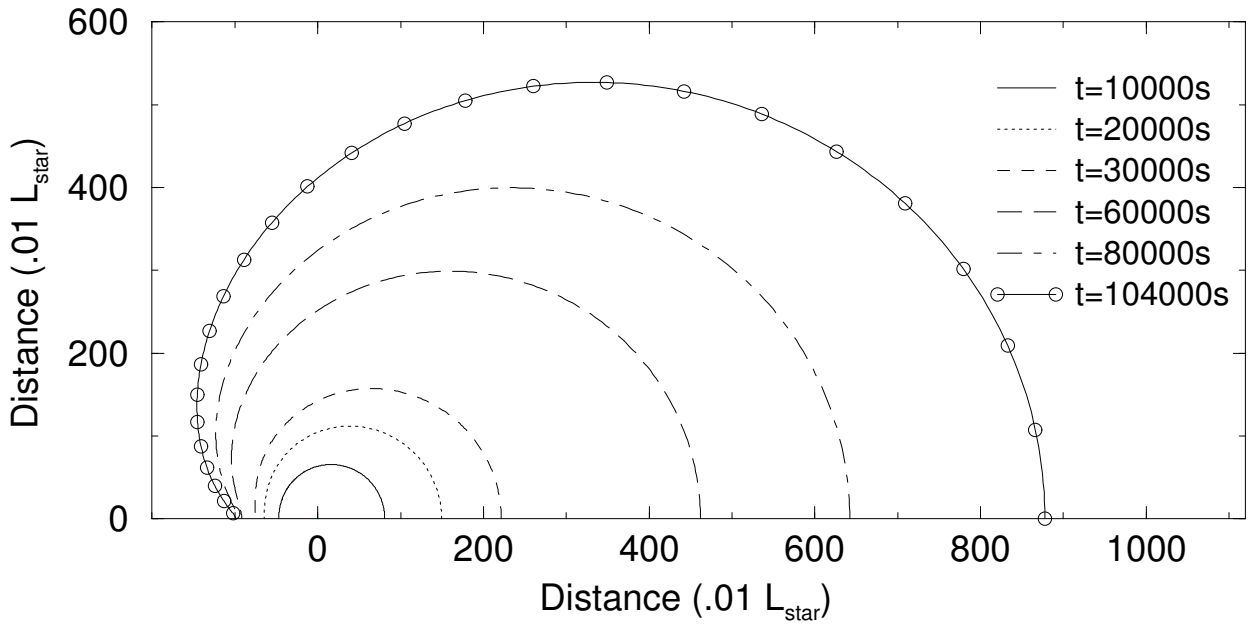

Fig. 1.— Bubble boundary vs. time for the fiducial case.

losses dominate. As early as 10s, all electrons with energies above 2×10^{-14}J have lost energy until they are all at this energy. For this calculation the initial spectrum was taken as very small so its influence is insignificant after <1s. The injection spectrum was taken as $Q(E) = 10^{37}(E/E_1)^{-1.5}J^{-1}s^{-1}$, which gives an electron injection rate integrated over energy of $10^{22}s^{-1}$ and an electron energy injection rate of $2 \times 10^{11}Js^{-1}$ for a maximum electron energy of $E_2 = 10^{-7}$J. Fig. 4 shows how the electron distribution, N(E,t) changes in the first few hundred seconds. Injection is resulting in a buildup of total number of electrons, but energy losses result in the electrons having lower energies. The major problem with the exact solution of the diffusion loss equation given here, is that only a finite range of electron energies are followed by the calculation. This range of energies drops rapidly with time to uninteresting values.

To cure the above problem, an approximate solution of the diffusion loss equation is made here, which is valid at higher energies. The results are shown in Fig. 4. The electron population increases slowly with time and has a slope of -2.5, except very near the lowest energies, where the approximation fails. Fig. 4 shows the resulting inverse Compton and synchrotron spectral luminosities vs. photon energy in SI units. The injection rate was chosen so that the observed X-ray flux (Leahy (2003)), for a distance to LSI +61°303 of 2kpc, agrees with the model luminosity. However the observed radio flux density is far below that from the model. This is because the synchrotron emission from the bubble is

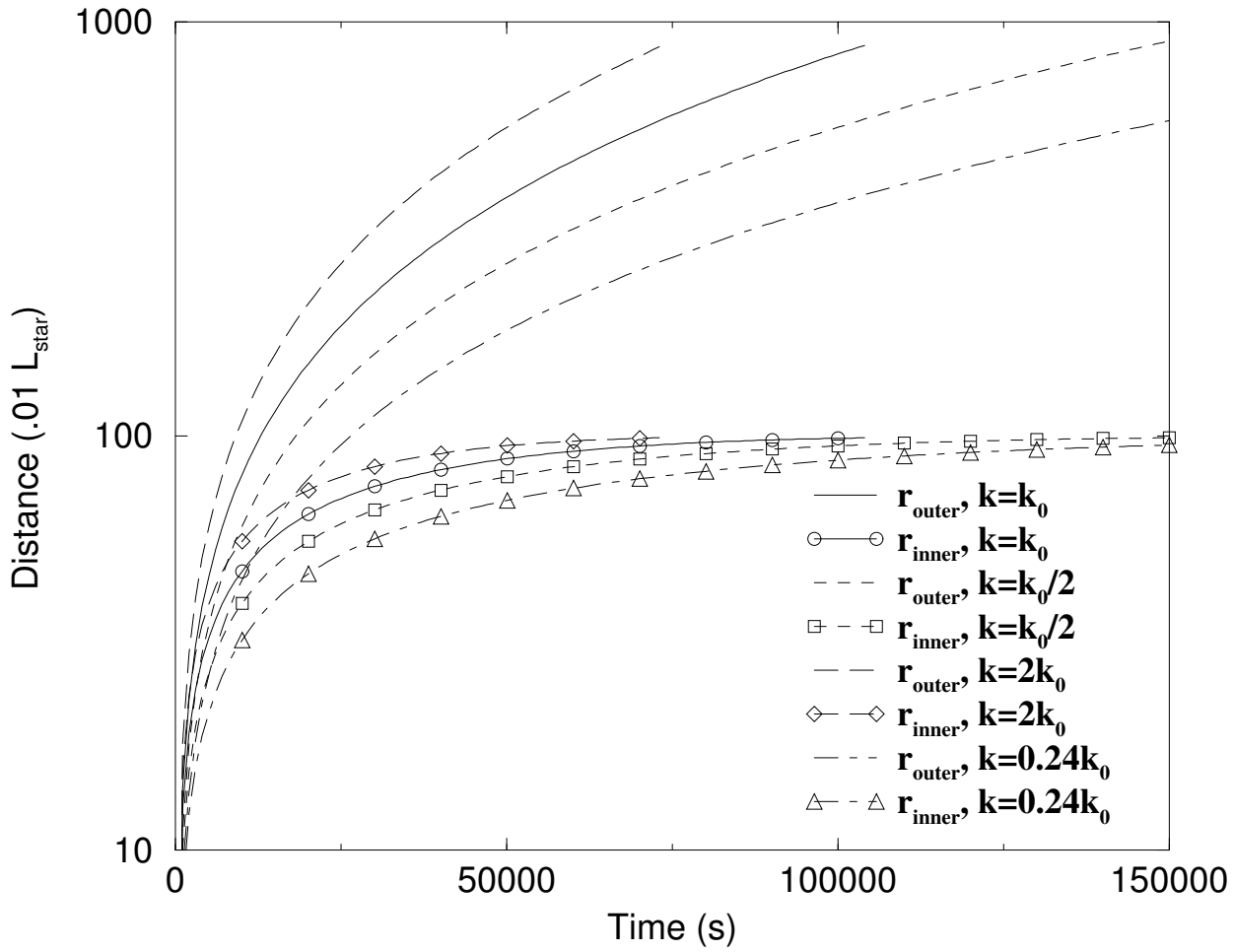

Fig. 2.— Inner and outer bubble distances from pulsar vs. time for the fiducial case ($k = k_0$) and other values of energy injection.

highly optically thick: the observed synchrotron is primarily optically thin and mainly from remnant electrons from previous radio outbursts (Leahy (2003)).

Since the synchrotron emission is optically thick, the synchrotron losses are drastically reduced and are much less than the inverse Compton losses. The calculation is redone omitting synchrotron losses. The resulting exact solution of the diffusion loss equation is shown in Fig. 4 for E vs. E0, and Fig. 4 for the electron distribution vs. current energy. The electron distribution drifts to lower energy at a significantly lower rate than for the case of optically thin synchrotron losses. Fig. 4 shows the approximate calculation for N, which is valid at higher energies. This yields an inverse compton luminosity similar to that

shown in Fig. 4, which agrees with observation. A calculation of the synchrotron radiation for the optically thick case is in progress. After that, a better calculation will be done for the electron distribution, which includes the exact solution at lower energies and the approximate solution at higher energies.

REFERENCES

Frail, D.A., Hjellming, R.M. 1991, AJ, 101, 2126

Harrison, F., Ray, P., Leahy, D., Waltman, E., Pooley, G. 2000, ApJ, 528, 454

Hutchings, J.B. and Crampton, D. 1981, Publ. Astr. Soc. Pacific, 93, 486

Leahy, D., Harrison, F., Yoshida, A. 1997, ApJ, 475, 823

Leahy, D.A. 2001, A&A, 380, 516

Leahy, D.A. 2003, A&A, 413, 1019

Marti, J., Paredes, J.M., 1995, A&A, 269, 249

Massi, M., Paredes, J.M., Estalella, R., and Felli, M. 1993, A&A, 269, 249

Paredes, J.M., Figueras, F., 1986, A&A, 154, L30

Ray, P., Foster, R., Waltman, E., Tavani, M., Ghigo, F., 1997 ApJ, 491, 381

Taylor, A.R., Gregory, P.C., 1984, ApJ, 283, 273

Waters, L.B.F.M., Taylor, A.R., van den Heuvel, E.P.J.m Habets, M.J.H., and Persi, P. 1988, A&A, 198, 200

This preprint was prepared with the AAS LaTeX macros v5.0.

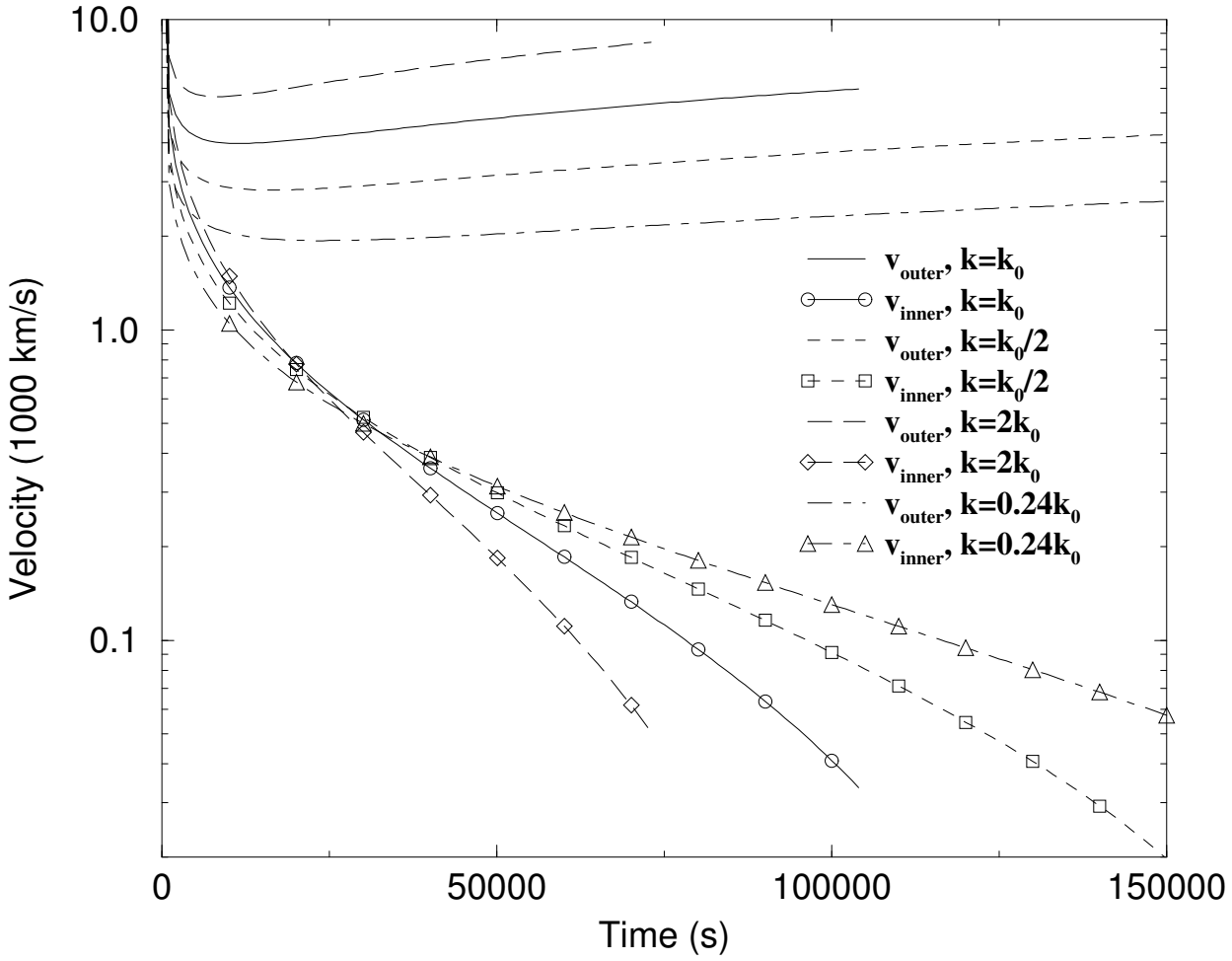

Fig. 3.— Inner and outer bubble velocities from pulsar vs. time for the fiducial case ($k = k_0$) and other values of energy injection.

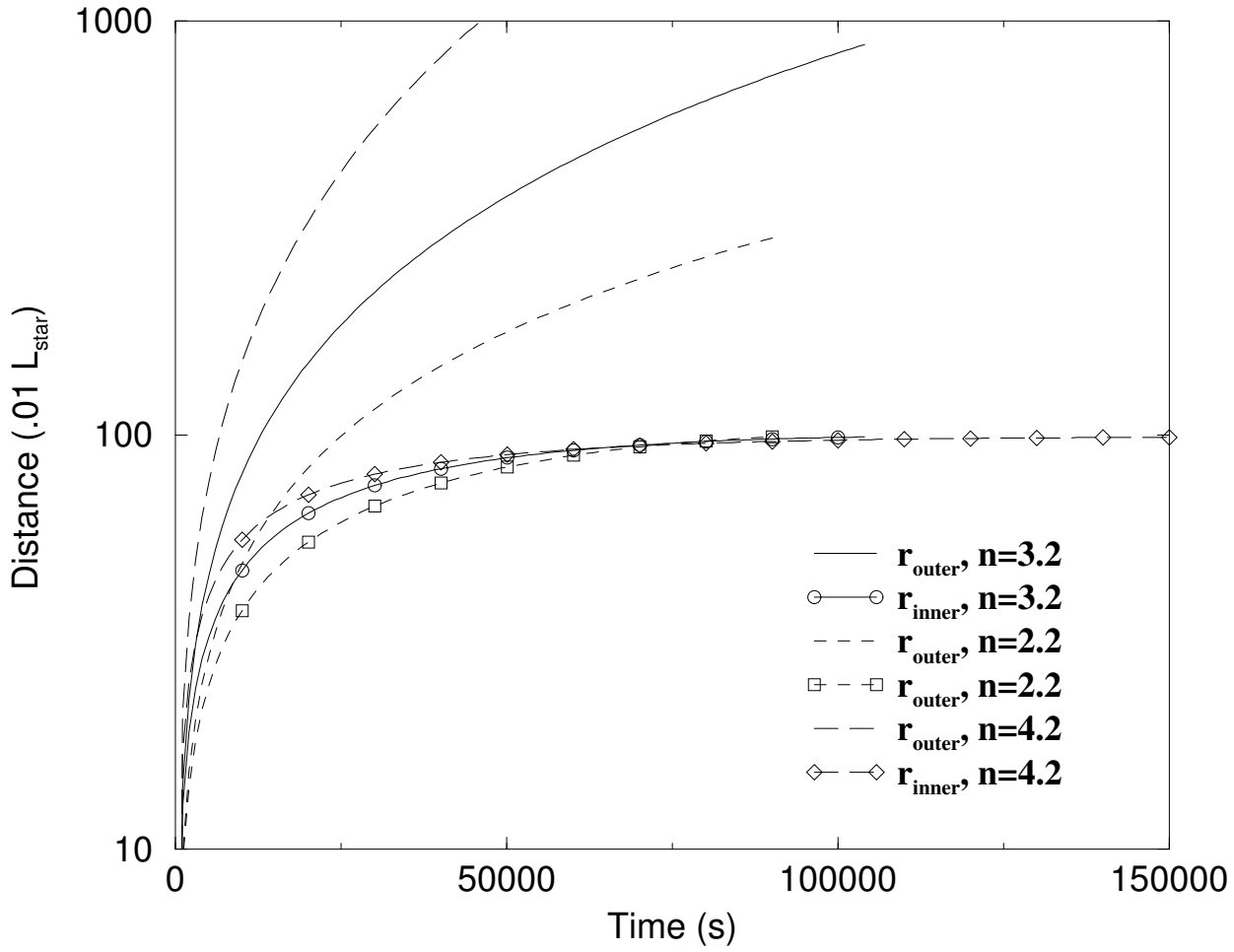

Fig. 4.— Inner and outer bubble distances from pulsar vs. time for the fiducial case ($n = 3.2$) and other values of density power-law.

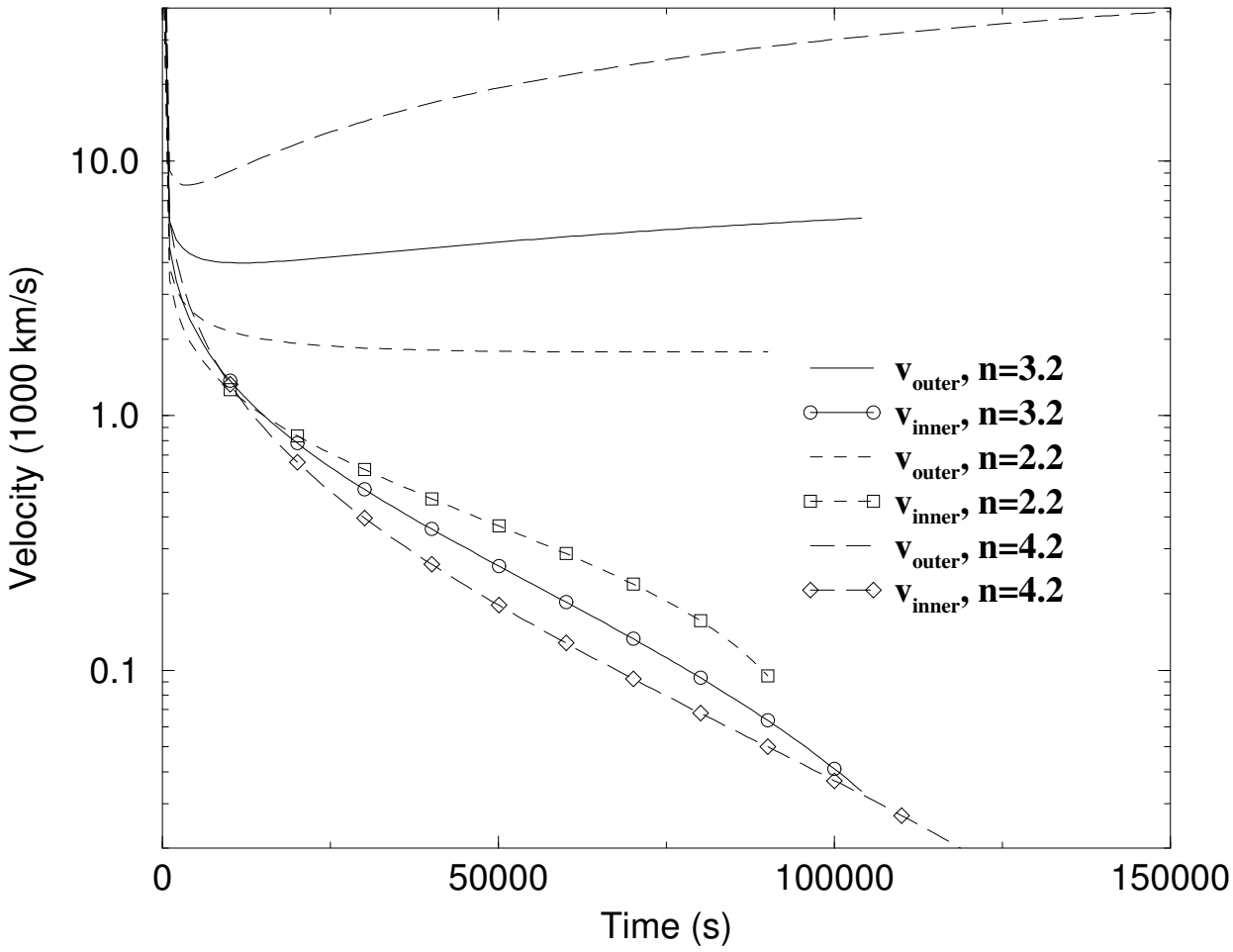

Fig. 5.— Inner and outer bubble velocities from pulsar vs. time for the fiducial case ($n = 3.2$) and other values of density power-law.

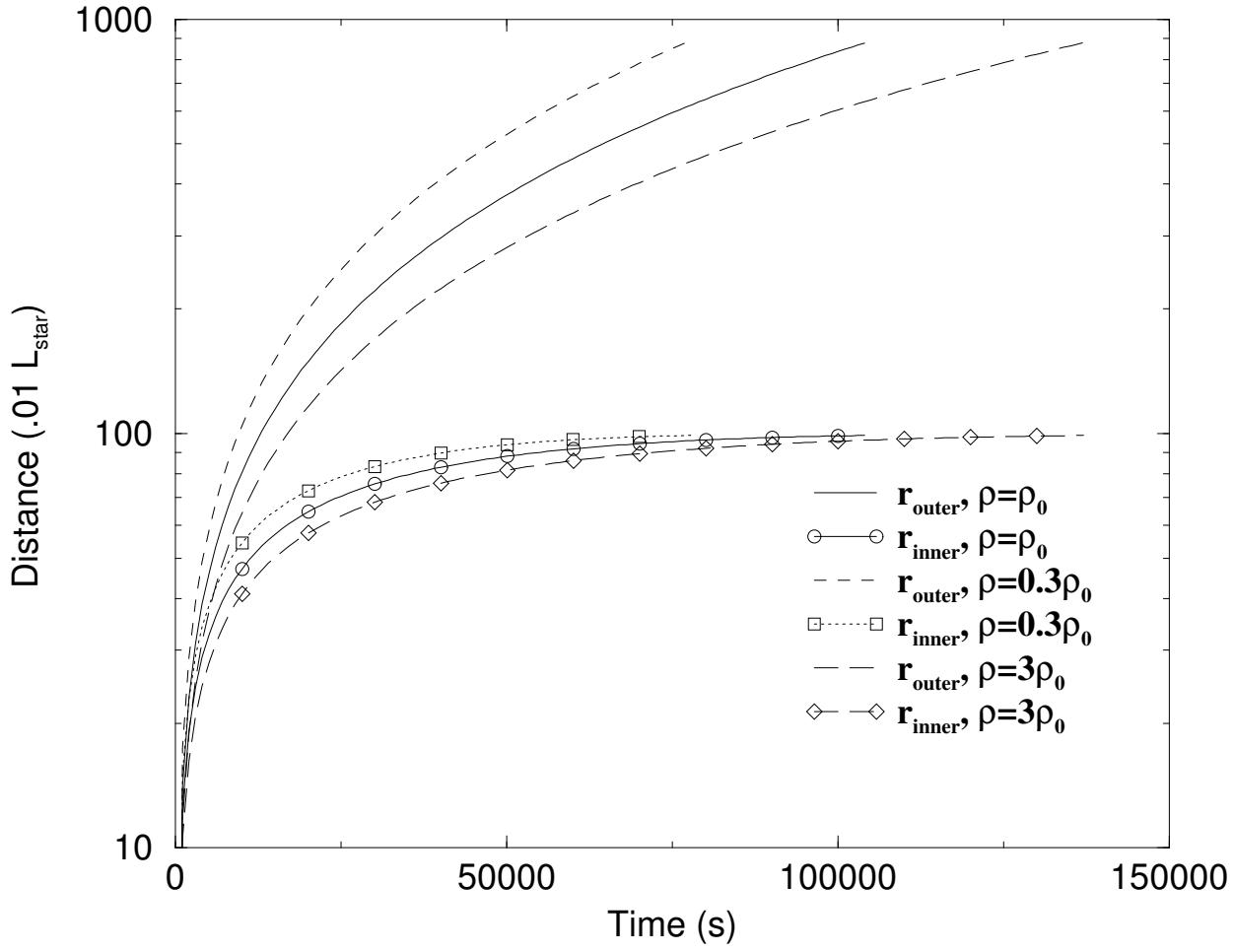

Fig. 6.— Inner and outer bubble distances from pulsar vs. time for the fiducial case ($\rho_0 = 10^{-8} kg/m^3$) and other values of density normalization.

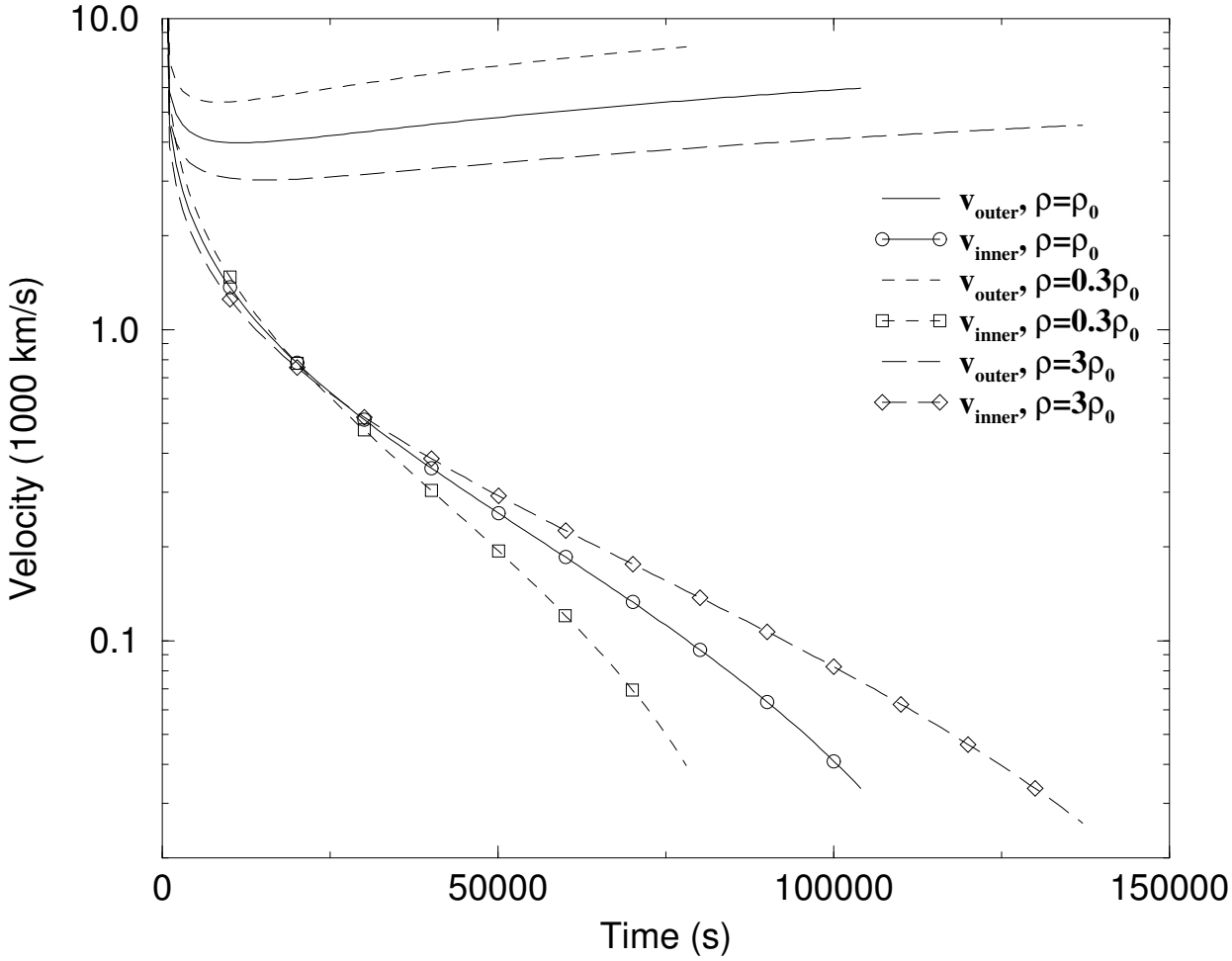

Fig. 7.— Inner and outer bubble velocities from pulsar vs. time for the fiducial case ($\rho_0 = 10^{-8} kg/m^3$) and other values of density normalization.

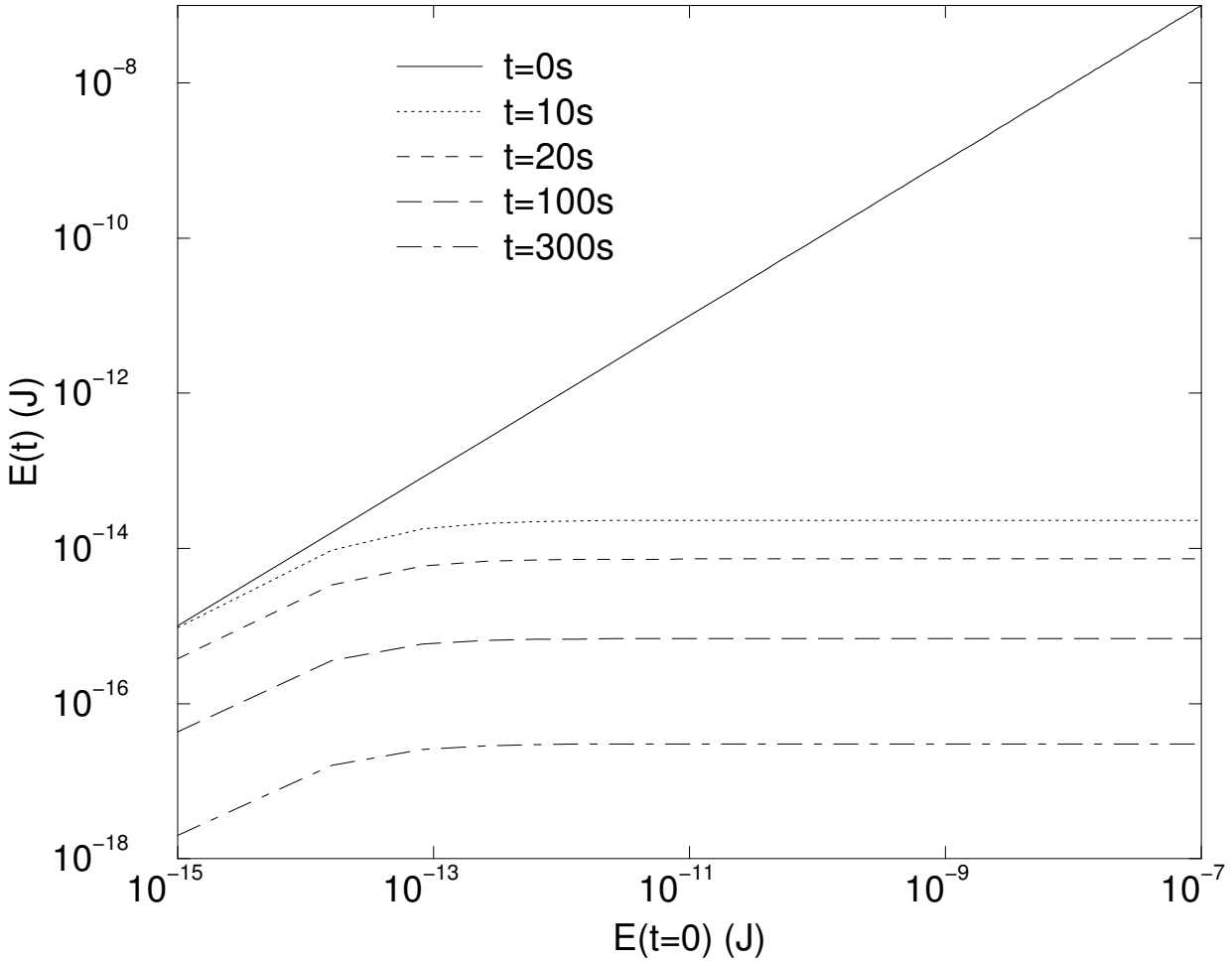

Fig. 8.— Electron energy vs. initial energy for several values of time, early in the bubble evolution.

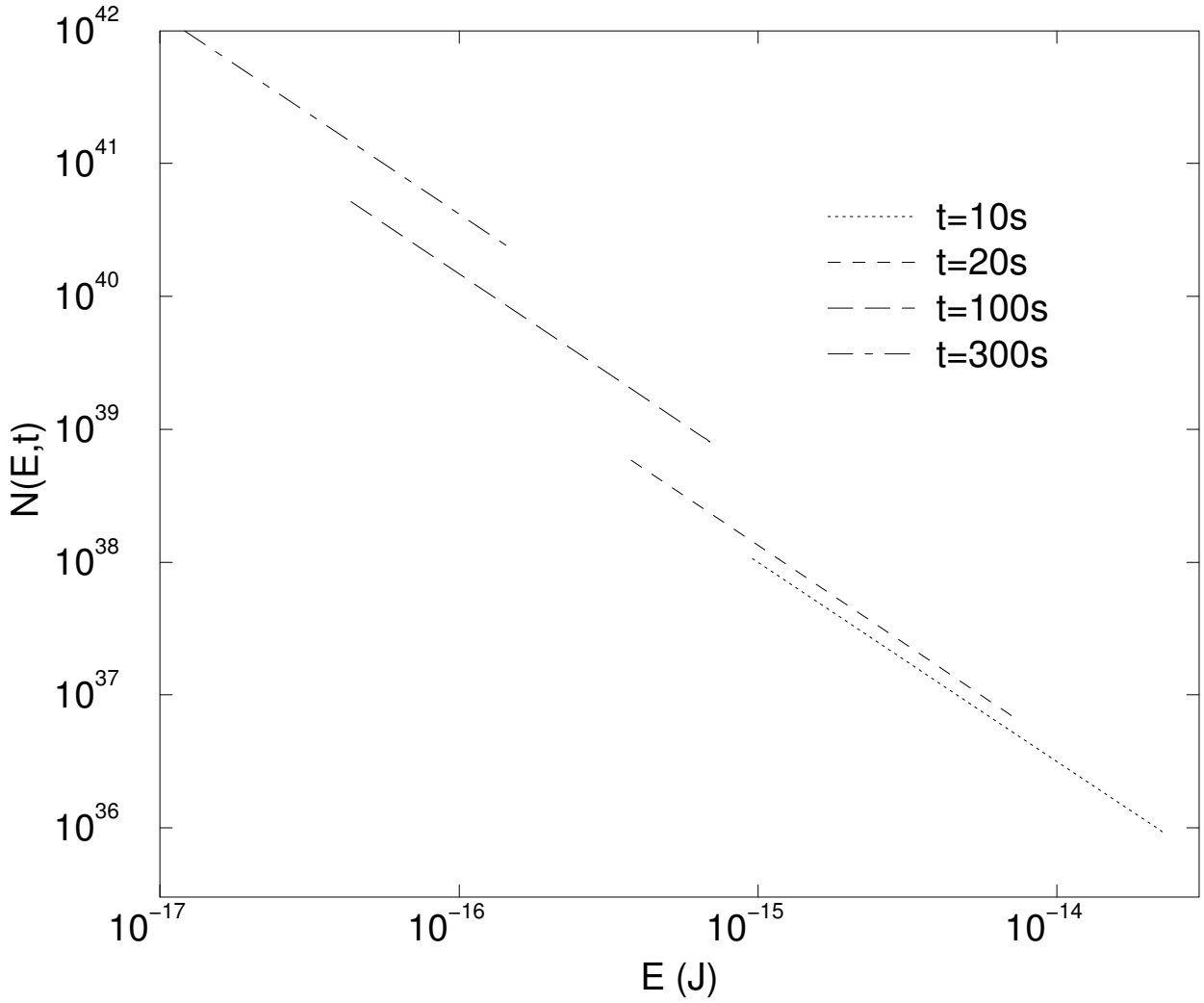

Fig. 9.— Electron distribution vs. current energy for several values of time.

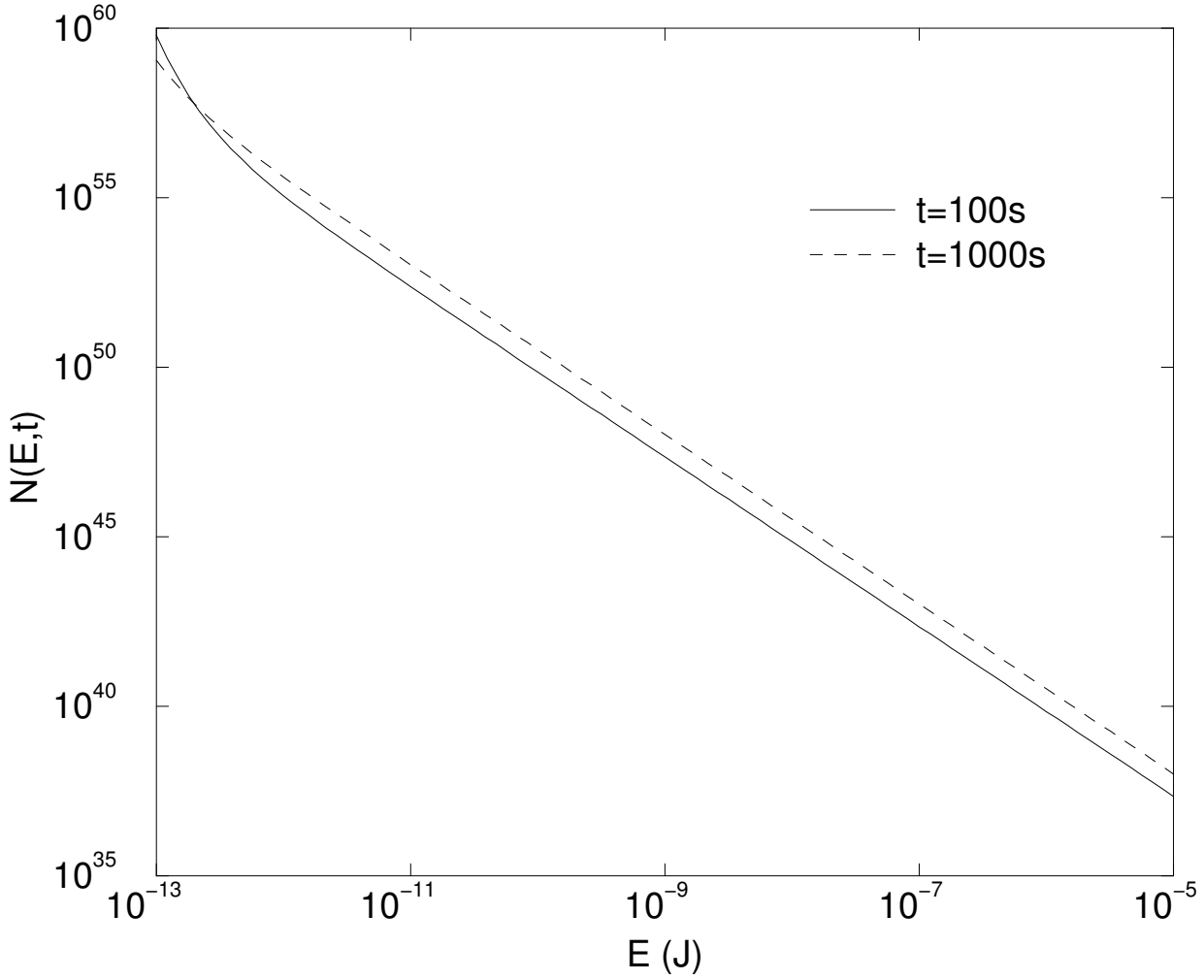

Fig. 10.— Electron distribution vs. current energy, using the approximation (see text).

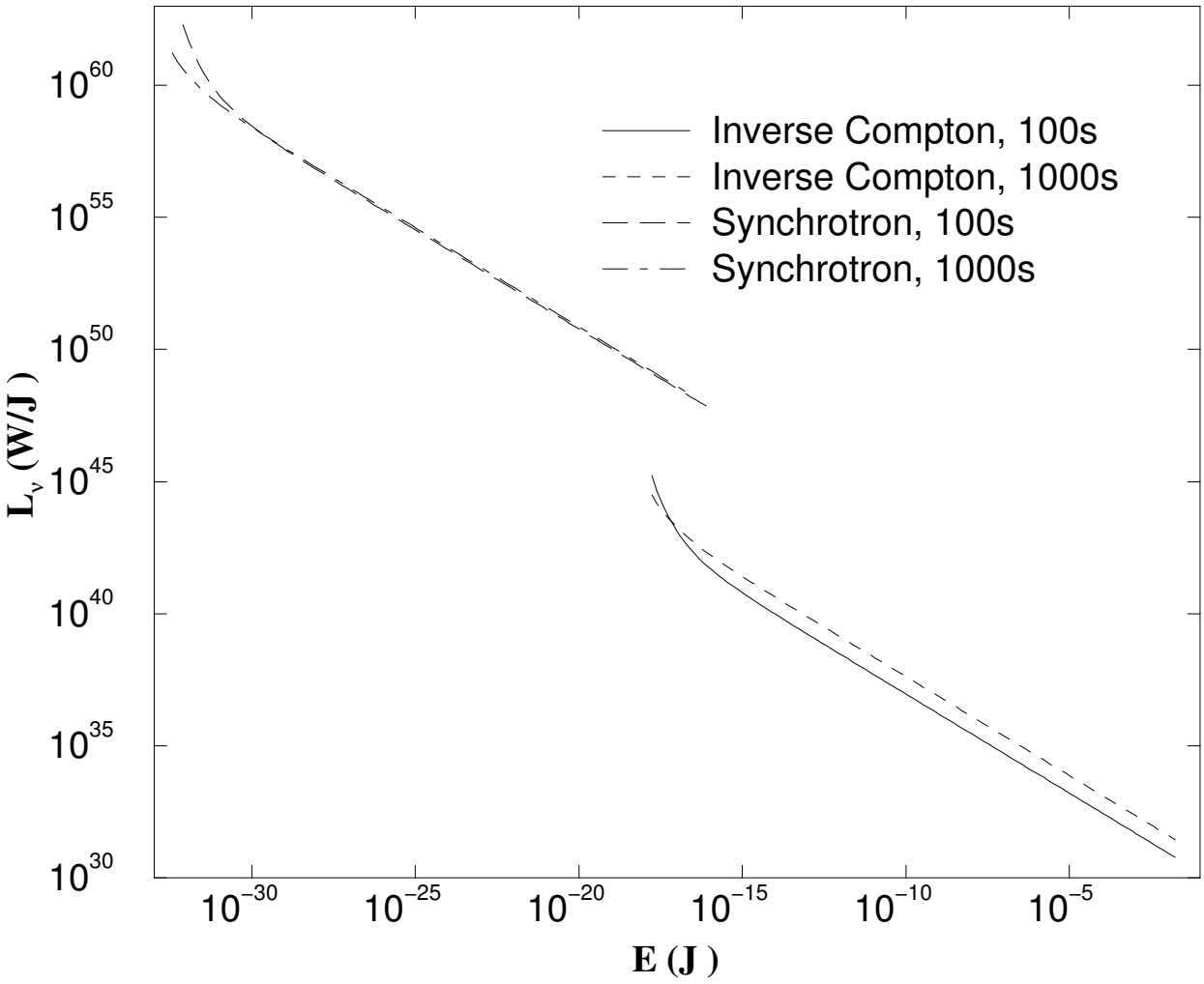

Fig. 11.— Photon luminosity vs. photon energy, using the approximation (see text).

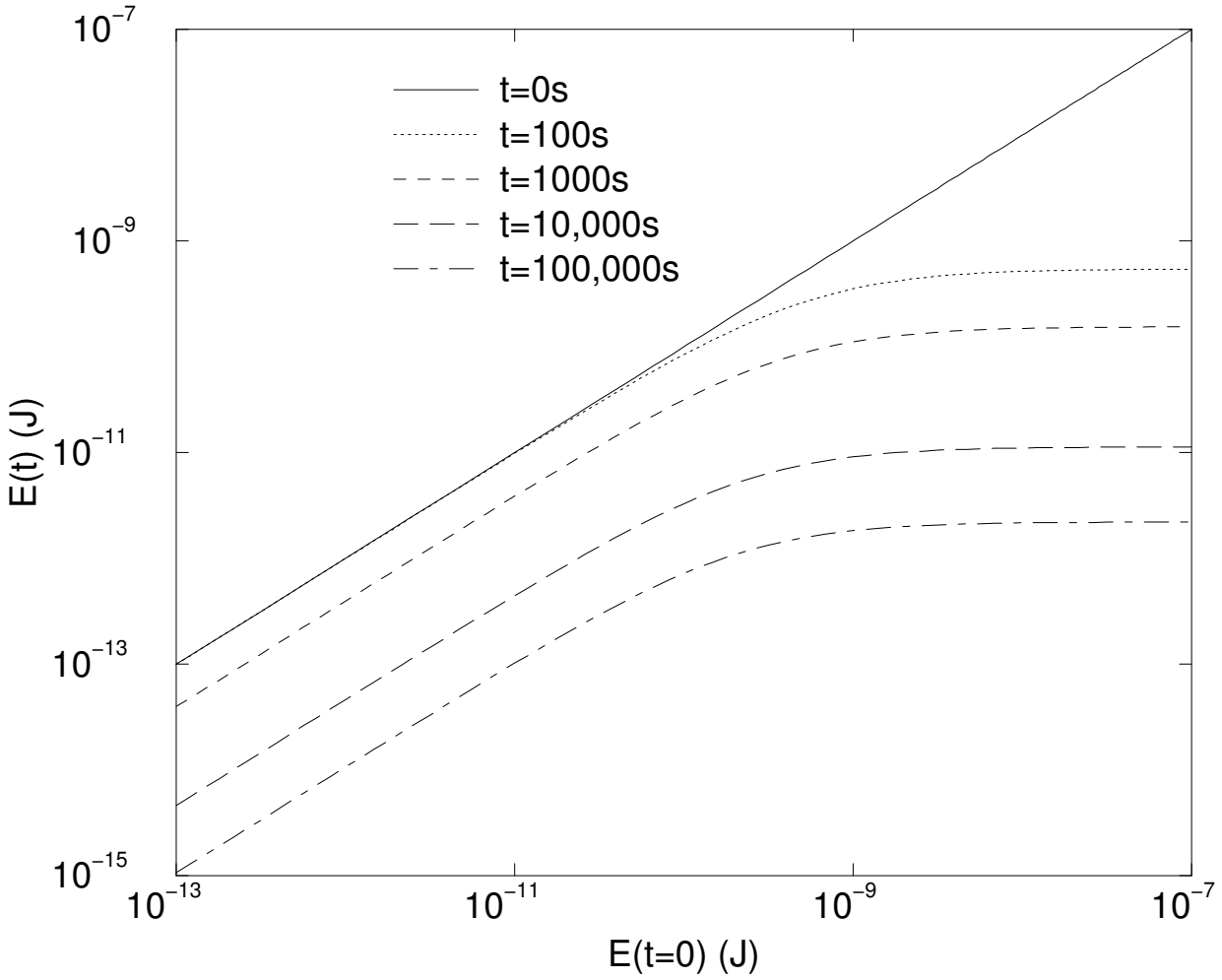

Fig. 12.— Electron energy vs. initial energy for several values of time, omitting synchrotron losses.

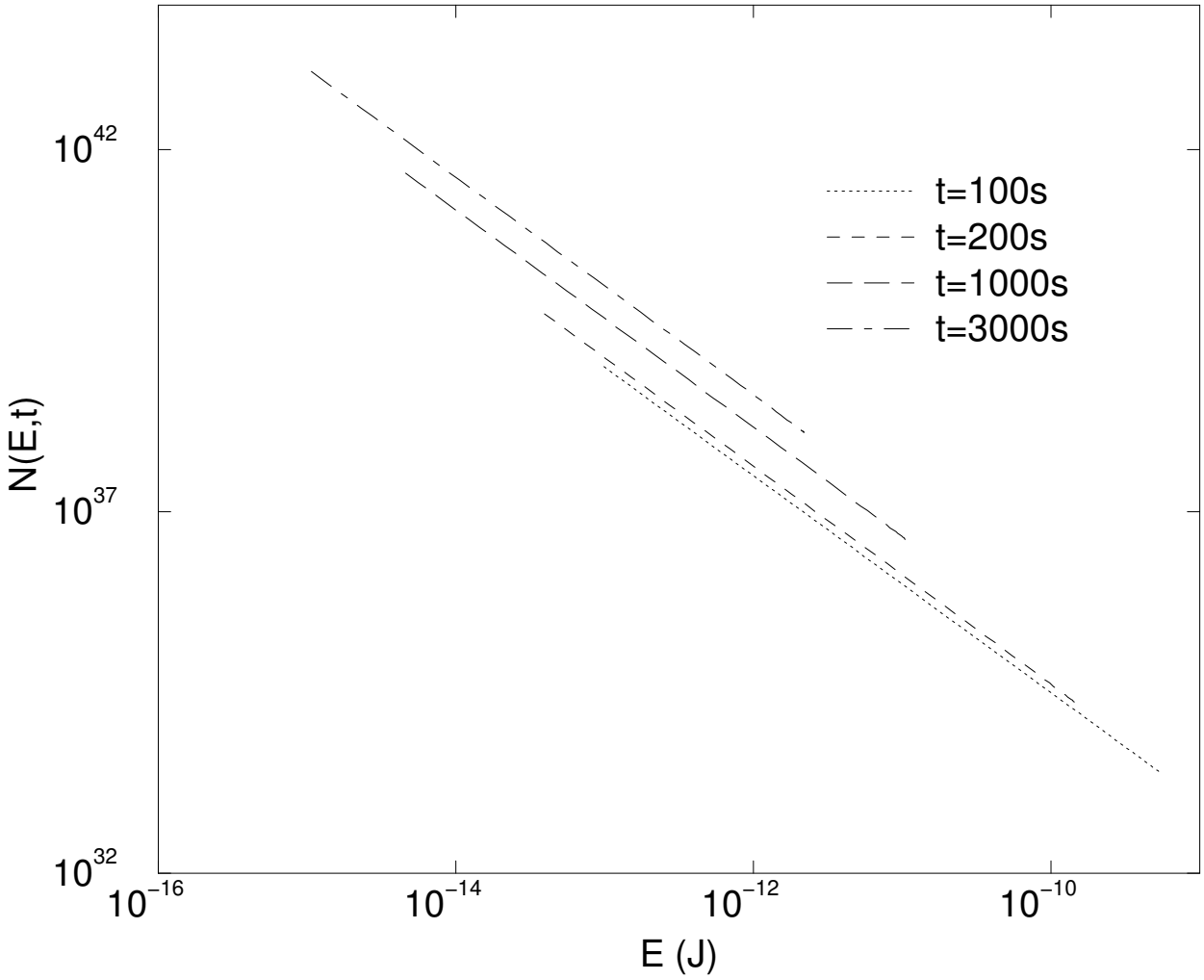

Fig. 13.— Electron distribution vs. current energy for case of no synchrotron losses.

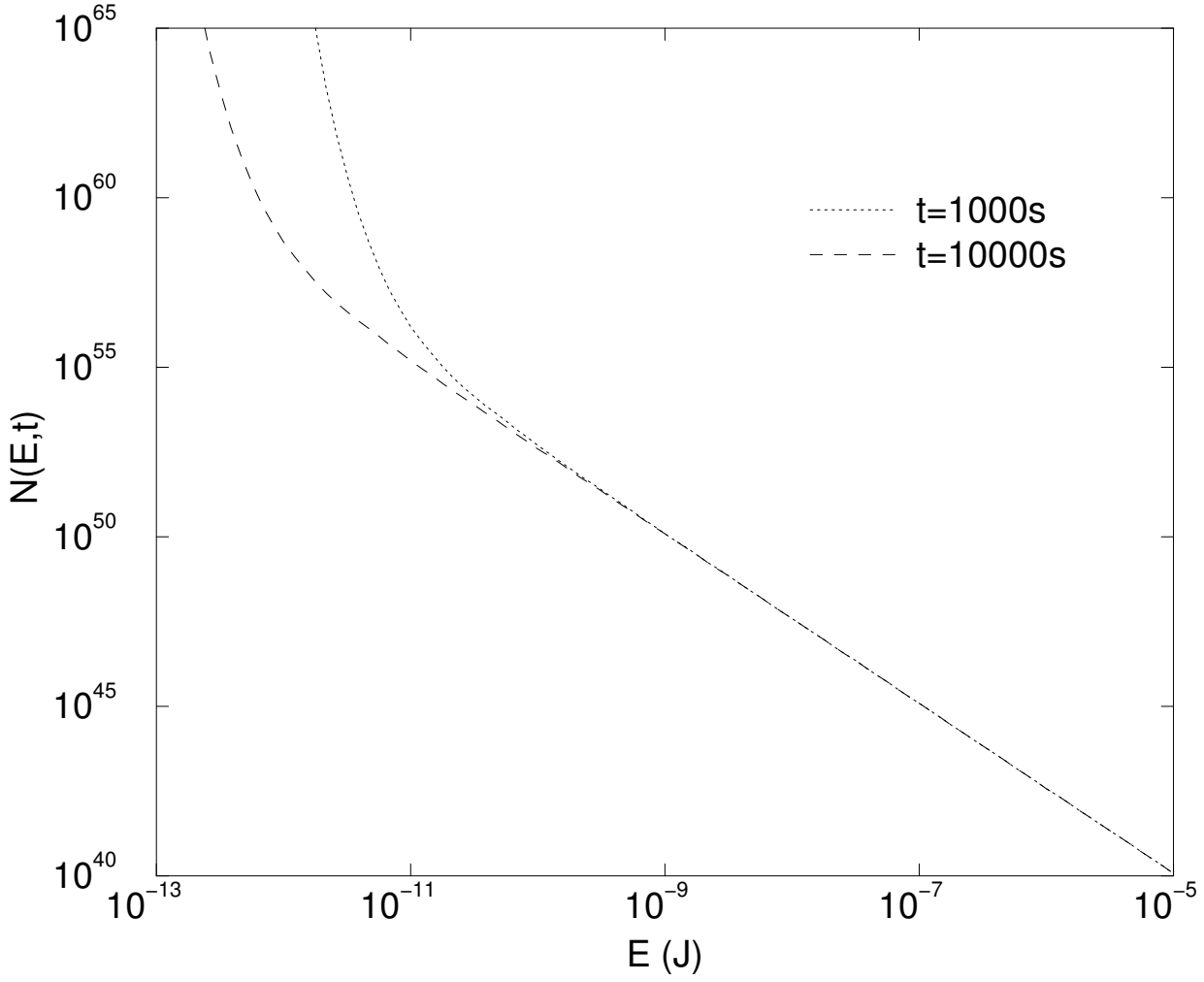

Fig. 14.— Electron distribution vs. current energy, using the approximation (see text).